

## RESEARCH ARTICLE

# Seasonal prediction of high-resolution temperature at 2-m height over Mongolia during boreal winter using both coupled general circulation model and artificial neural network

Gerelchuluun Bayasgalan  | Joong-Bae Ahn 

Division of Earth Environmental System, Pusan National University, Busan, South Korea

## Correspondence

Joong-Bae Ahn, Division of Earth Environmental System, Pusan National University, Jangjeon 2-dong, Geumjeong-gu, Busan 609-735, South Korea.

Email: jbahn@pusan.ac.kr

## Funding information

Rural Development Administration, Grant/Award Number: KMI2018-01213; Korean Meteorological Administration, Grant/Award Number: PJ01229302

The hindcast data of Pusan National University coupled general circulation model (PNU CGCM), a participant model of the Asia-Pacific Economic Cooperation Climate Center (APCC) Multi-Model Ensemble Climate Prediction System, and August–October sea-surface temperature (SST) in the northern Barents–Kara Sea (BKI) and the sea-ice extent (SIE) in the Chukchi Sea (East Siberian Sea index [ESI]) are used for predicting  $20 \times 20$ -km-resolution anomalous surface air temperature at 2-m height (aT2m) over Mongolia for boreal winter. For this purpose, area-averaged surface air temperature (TI) and sea-level pressure (SLP) over Mongolia are defined. Then four large-scale indices,  $TI_{\text{mdl}}$  and  $SHI_{\text{mdl}}$  obtained from PNU CGCM, and  $TI_{\text{MLR}}$  and  $SHI_{\text{MLR}}$  obtained from multiple linear regressions on BKI and ESI, are incorporated using the artificial neural network (ANN) method for the prediction and statistical downscaling to obtain the monthly and seasonal  $20 \times 20$ -km-resolution aT2m over Mongolia in winter. An additional statistical method, which uses BKI and ESI as predictors of TI and SHI together with dynamic prediction by the CGCM, is used because of the relatively low skill of seasonal predictions by most of the state-of-the-art models and the multi-model ensemble systems over high-latitude landlocked Eurasian regions such as Mongolia. The results show that the predictabilities of monthly and seasonal  $20 \times 20$ -km-resolution aT2m over Mongolia in winter are improved by applying ANN to both statistical and dynamical predictions compared to utilizing only dynamic prediction. The predictability gained by the proposed method is also demonstrated by the probabilistic forecast implying that the method forecasts aT2m over Mongolia in winter reasonably well.

## KEYWORDS

artificial neural network, coupled general circulation model, Mongolian temperature, seasonal prediction

## 1 | INTRODUCTION

The climate of Mongolia, a landlocked country located in the middle of the Asia, is characterized by a short dry summer and a long severe cold winter (MARCC, 2009). The winter climate is mainly influenced by the Siberian high (SH; e.g., Mijiddorj, 1999; Panagiotopoulos *et al.*, 2005),

which is a dominant circulation system over the Eurasian continent in winter. During this season, a severe cold surge named Dzud often hits Mongolia and causes extensive damage, mainly to livestock. Dzud prevents the livestock from grazing, leading to starvation (Chogsom, 1964; Namkhai and Mijiddorj, 1986; Natsagdorj, 2000). In Mongolia, although heavy snows are rare, cold surges are more

frequent in winter (Natsagdorj and Dulamsuren, 2001). Among the natural disasters occurring in Mongolia, loss of livestock due to Dzud is the most overwhelming. Total livestock losses due to Dzud from 2004 to 2015 exceeded 10 million according to the National Agency for Meteorology and Environmental Monitoring (NAMEM). During this 12-year period, Dzud accounted for 92% of the total natural disasters in Mongolia and caused enormous socio-economic damage in Mongolia due to the economy's strong dependence on the livestock industry. Seasonal forecasting over the region is, therefore, vitally important for stock farmers and government decision makers to prepare for the severe cold waves such as Dzud in the forthcoming winter.

Seasonal forecasting by numerical modelling is limited because of the atmosphere's chaotic nature (e.g., Derome *et al.*, 2005) and the complexity of the climate system (e.g., Ahn and Lee, 2016). Particularly, climate prediction over inland continental regions such as Mongolia is one of the most challenging issues for state-of-the-art meteorology due to the limitations of current observation that hinder our understanding of the interaction between land surface and atmosphere and due to the difficulties in modelling the complex and inhomogeneous distribution of the terrestrial surface in detail.

Meehl (1995) claimed that the coupled general circulation model (CGCM) is the ultimate tool for predicting the long-term weather and climate. Thus, in spite of their relatively low climate prediction skill over continents, state-of-the-art CGCMs are still widely used for seasonal forecasting in many meteorological research centres and laboratories, such as the National Centers for Environmental Prediction (NCEP; Toth *et al.*, 2001), the European Centre for Medium-Range Weather Forecast (ECMWF; Anderson *et al.*, 2007), the Asia-Pacific Economic Cooperation Climate Center (APCC; Lee *et al.*, 2013; Lee *et al.*, 2014) and Pusan National University (PNU; Sun and Ahn, 2014; Kim and Ahn, 2015).

Even though the horizontal resolutions of CGCMs are relatively coarse compared to regional climate models, in general, CGCMs can present the local climate to some extent because they are believed to capture the general features of the observed continental-scale atmospheric circulation patterns (e.g., Ahn and Kim, 2014; Scaife *et al.*, 2014; Sun and Ahn, 2014). Hence, the CGCM outputs can be localized into the regional scale using dynamical (e.g., Im *et al.*, 2008; Battbold *et al.*, 2011) or statistical downscaling techniques such as multiple linear regression (MLR), canonical correlation analysis and singular value decomposition (Wilks, 1995; Henrik *et al.*, 1999; Schoof and Pryor, 2001; Sun and Chen, 2012), as well as artificial neural networks (ANN; Schoof and Pryor, 2001; Coulibaly and Dibike, 2005) and genetic algorithms (Ahn and Lee, 2016).

In this study, the ANN method is applied to the hindcast data of PNU CGCM and to the proceeding autumn sea-surface temperature (SST) and sea-ice extent (SIE) which

strongly affect the subsequent winter climate of Mongolia for the downscaled prediction of the  $20 \times 20$ -km-resolution monthly mean air temperature at 2-m height (T2m) over Mongolia in winter. This statistical method is used to correct the CGCM prediction using statistical correlation between the predictor of the proceeding season and Mongolian winter temperature, as well as to downscale the coarse resolution surface temperature to a high-resolution one.

Section 2 introduces the study data. Section 3 describes the large-scale climate indices and factors affecting the Mongolian winter climate. Section 4 introduces the method to produce high-resolution boreal winter temperature prediction using various climate indices obtained from CGCM prediction and observation. The results and verification of the prediction are presented in section 5. Finally, the summary and conclusion are provided in section 6.

## 2 | DATA

The monthly data of the National Centers for Environmental Protection/National Center for Atmospheric Research (NCEP/NCAR) reanalysis (hereafter RA2) spanning 1981–2015 (Kanamitsu *et al.*, 2002) were used as observations. To reconcile the horizontal resolution of RA2 to PNU CGCM outputs, RA2 is regridded using ESMF\_regrid (NCL, 2016).

Monthly mean  $20 \times 20$ -km-resolution T2m over Mongolia produced by Gerelchuluun and Ahn (2014) is utilized as the reproduced observation. Following Gerelchuluun and Ahn (2014), the data are downscaled from coarse resolution of RA2 to  $20 \times 20$  km resolution by using a dynamical and statistical method considering the effect of temperature inversion. Specifically, the systematic bias induced by dynamical downscaling simulated by the Weather Research and Forecasting (WRF) model with the boundary condition of RA2 is corrected by using a statistical method. Considering that the bias can be divided into the mean and perturbation parts (Ahn *et al.*, 2012), the former is corrected using a weighting function with a so-called “inversion correction” that considers the effect of temperature inversion when the inversion occurs in the lower atmosphere. The perturbation part of the bias is corrected by using the self-organizing maps (SOM) method. For more detail, refer to Gerelchuluun and Ahn (2014).

The observed monthly mean SST and SIE are extracted from the Research Data Archive at the NCAR for the period 1981–2015 (Rayner *et al.*, 2006). In particular, autumn SST and SIE in the northern Kara Sea and Chukchi Sea, respectively, are used for predicting the large-scale climate indices, together with the CGCM prediction data.

Ten-ensemble mean monthly averaged PNU CGCM hindcast data are used for the boreal winter climate of Mongolia. The PNU CGCM, having T42 spectral horizontal resolution for the atmospheric component and  $0.7^\circ$ ,  $1.4^\circ$  and  $2.8^\circ$  resolutions in the meridional direction below  $30^\circ$ , at

mid-latitude ( $30^{\circ}$ – $60^{\circ}$ ) and at higher latitudes ( $>60^{\circ}$ ) for the oceanic component, respectively, is used to generate 3-month lead hindcasts. A detailed description of PNU CGCM, a participant model of the APCC multi-model ensemble climate prediction (Ahn and Kim, 2014; Sun and Ahn, 2014; Kim and Ahn, 2015), is presented in Kim and Ahn (2015). The ensemble members are produced based on a time-lagged method (Brankovic *et al.*, 1990) and the initial conditions of each ensemble member are taken from 10 different days of November of each year from 1981 to 2014 for December ( $\sim 0.5$  month lead), January ( $\sim 1.5$  month lead) and February ( $\sim 2.5$  month lead) predictions. The integrations are performed at both PNU and NAMEM.

### 3 | LARGE-SCALE INDICES AND MONGOLIAN CLIMATE

Winter mean T2m and sea-level pressure (SLP) for 1981–2015 are shown in Figure 1. Although the regional distribution of T2m over Mongolia is complex and highly nonlinear (Gerelchuluun and Ahn, 2014), the local climate condition is mainly influenced by and related to the large-scale climate (Orlanski, 1975; Wigley *et al.*, 1990). Thus, in an attempt to relate the large-scale climate variability to the local scale one, the area-averaged T2m ( $87^{\circ}$ – $121^{\circ}$ E and  $40^{\circ}$ – $53^{\circ}$ N) and mean SLP ( $80^{\circ}$ – $120^{\circ}$ E and  $40^{\circ}$ – $65^{\circ}$ N; see

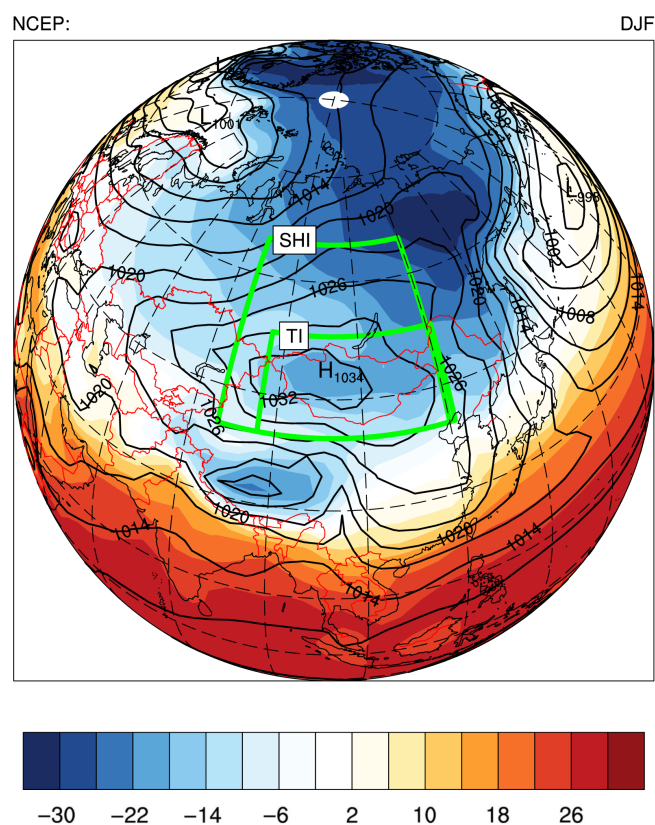


**FIGURE 1** Winter climatologies of T2m (colour,  $^{\circ}$ C) and SLP (contour, hPa) from observation (1981–2015). Rectangle areas indicate domains for TI and SHI [Colour figure can be viewed at [wileyonlinelibrary.com](http://wileyonlinelibrary.com)]

Figure 1) are defined as the temperature index (TI) and the SH index (SHI), respectively. These indices are used for the statistically downscaled  $20 \times 20$ -km-resolution T2m.

#### 3.1 | Temperature index

The area-averaged T2m from RA2 is defined as the observed air temperature index ( $TI_{obs}$ ). The ensemble mean of hindcasted T2m from PNU CGCM averaged over the same domain is also defined as  $TI_{mdl}$ .

Figure 2 shows the horizontal distribution of the simple linear regression (SLR) coefficient of monthly mean T2m anomaly ( $aT2m$ ) on  $20 \times 20$  km resolution over Mongolia against  $TI_{obs}$  during the winters of 1981/1982–2014/2015. According to the figure, all of the coefficients are statistically significant ( $p < .01$ ), except some areas in the eastern parts of Mongolia during December and January ( $p < .05$ ). In addition, the area-averaged coefficients of determinant based on SLR for each month and boreal winter (DJF) are between 0.55 and 0.74, indicating that more than half of the total area-averaged variation in  $aT2m$  over Mongolia during DJF and individual months can be largely explained by the linear relationship with  $TI_{obs}$ .

#### 3.2 | SH index

The SH, as shown in winter mean SLP of Figure 1, is a large-scale high-pressure system over the Eurasian continent centred at around Mongolia. As for the potential roles of the SH in winter climate over Asia, Ding and Krishnamurti (1987) and Park *et al.* (2014) attributed the severe cold waves to the SH and its movement to the cold surges intruding into the lower latitudes, generating stormy weather in southern China, the Indochina Peninsula, the Maritime Continent and the Southern Hemisphere tropics (Chang *et al.*, 2003; 2005). Following Panagiotopoulos *et al.* (2005) and Wu *et al.* (2006), the SHI from RA2 ( $SHI_{obs}$ ) is defined by averaging monthly mean SLP over the area ( $80^{\circ}$ – $120^{\circ}$ E and  $40^{\circ}$ – $65^{\circ}$ N; see Figure 1) and normalized by one standard deviation for the winters of 1981/1982–2014/2015. The ensemble mean of hindcasted SLP from PNU CGCM averaged over the same domain is also defined as  $SHI_{mdl}$ .

The SLR coefficients of  $20 \times 20$  km  $aT2m$  against  $SHI_{obs}$  are illustrated in Figure 3. Except in the northeastern part of Mongolia, the coefficients are overall statistically significant ( $p < .05$ ). In addition, approximately 35–43% of the area-averaged total variation of  $aT2m$  over Mongolia is explained by  $SHI_{obs}$ . This implies that the regional variance of  $20 \times 20$  km  $aT2m$  over Mongolia can be represented reasonably well by both  $SHI_{obs}$  and  $TI_{obs}$ .

#### 3.3 | Arctic impact on Mongolian climate: Statistical correction

The predictability of dynamical models is mostly due to their high skill level in the tropics (Derome *et al.*, 2005; Lin

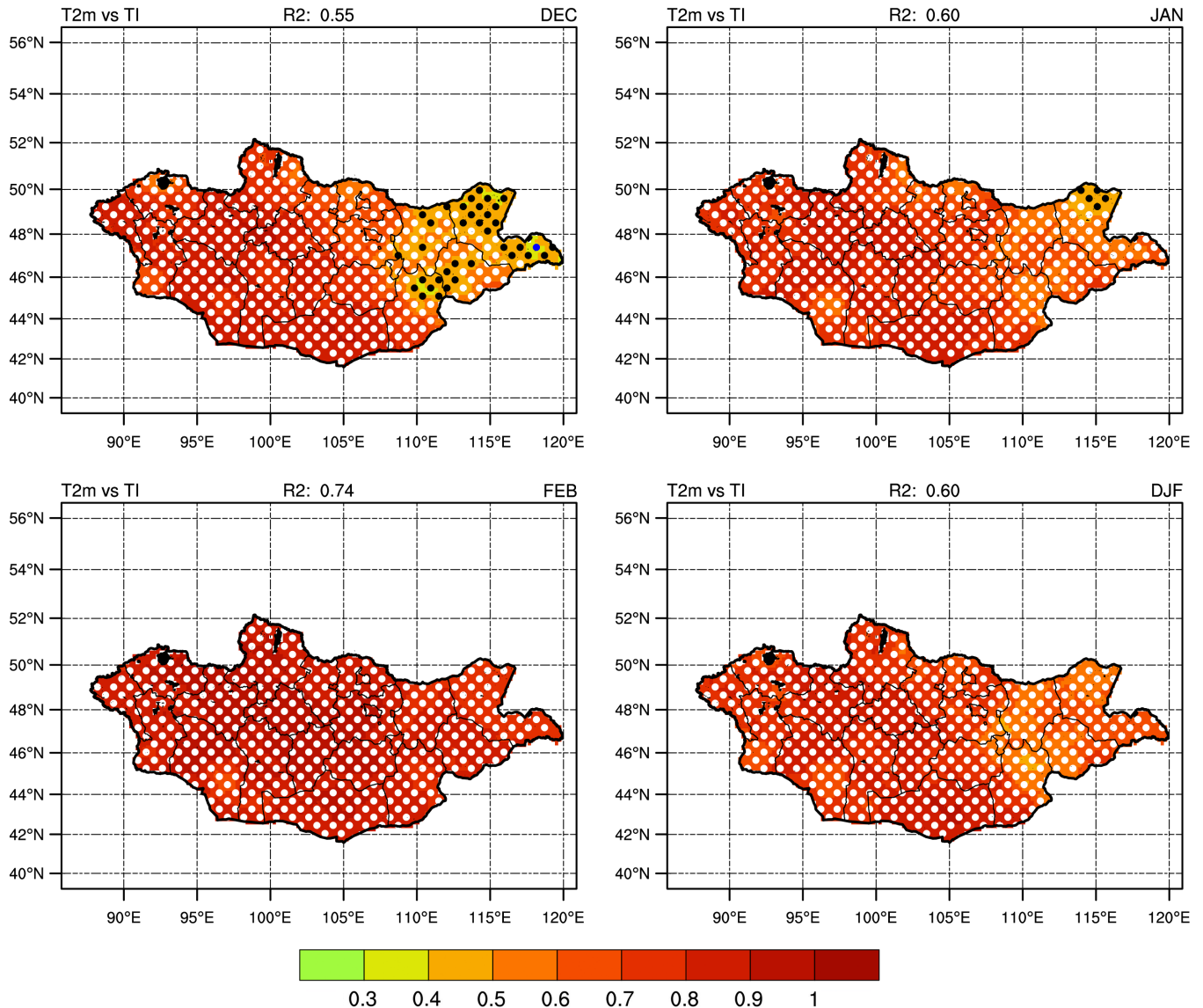


**FIGURE 2** Regression of aT2m (20 × 20 km grid) on  $TI_{obs}$  stippling with colours indicates statistical significances at 90% (green), 95% (black) and 99% (white) levels. R2 means the area-averaged coefficient of determinant [Colour figure can be viewed at [wileyonlinelibrary.com](http://wileyonlinelibrary.com)]

*et al.*, 2005; Kim and Ahn, 2015). Most models have relatively good skill in predicting tropical SST anomalies, particularly equatorial Pacific SST anomalies. However, the skill of seasonal predictions by most of the state-of-the-art models and multi-model ensemble systems over the central Asia region (Min *et al.*, 2014; Kim *et al.*, 2016) is relatively low. Thus, the dynamic prediction needs to be corrected statistically, considering our current predictability over the high-latitude landlocked Eurasian region such as Mongolia.

Many studies have pointed out the significance of the Arctic impact on the northern Eurasia climate variability. Particularly, it has been shown that a decrease in the autumn East Arctic SIE tends to strengthen the SH and East Asia winter monsoon (e.g., Honda *et al.*, 2009; Wu *et al.*, 2011). Also, several studies (e.g., Hall *et al.*, 2015; Kryjov, 2015) have claimed that the autumn positive SST anomalies in the East Arctic tend to be followed by the negative phase of the

Arctic Oscillation, an enhanced SH and negative temperature anomalies in the northern Eurasia in winter.

Climatological SIE in the boreal early autumn (August, September and October [ASO]; Figure 4a) and correlation coefficients between observed ASO SST and DJF  $TI_{obs}$  (Figure 4b) and  $SHI_{obs}$  (Figure 4c), and the correlation coefficients between observed ASO SIE in the Arctic Sea and DJF  $TI_{obs}$  (Figure 4d) and  $SHI_{obs}$  (Figure 4e) are shown in Figure 4. Figure 4b,c,d,e indicates that winter  $TI_{obs}$  and  $SHI_{obs}$  are, respectively, significantly related with ASO SST (ASO SIE) linearly in the northern Kara Sea and Chukchi Sea, the areas adjacent to the sea ice margin (Figure 4a). In particular, ASO SST is closely related with both DJF  $TI_{obs}$  and  $SHI_{obs}$  in the area A (75°–82°N and 34°–94°E), and ASO SIE is closely related with both DJF  $TI_{obs}$  and  $SHI_{obs}$  in the area P (73°–79°N and 170°E–160°W). The area A is climatologically opened from ice during ASO, while the area P is

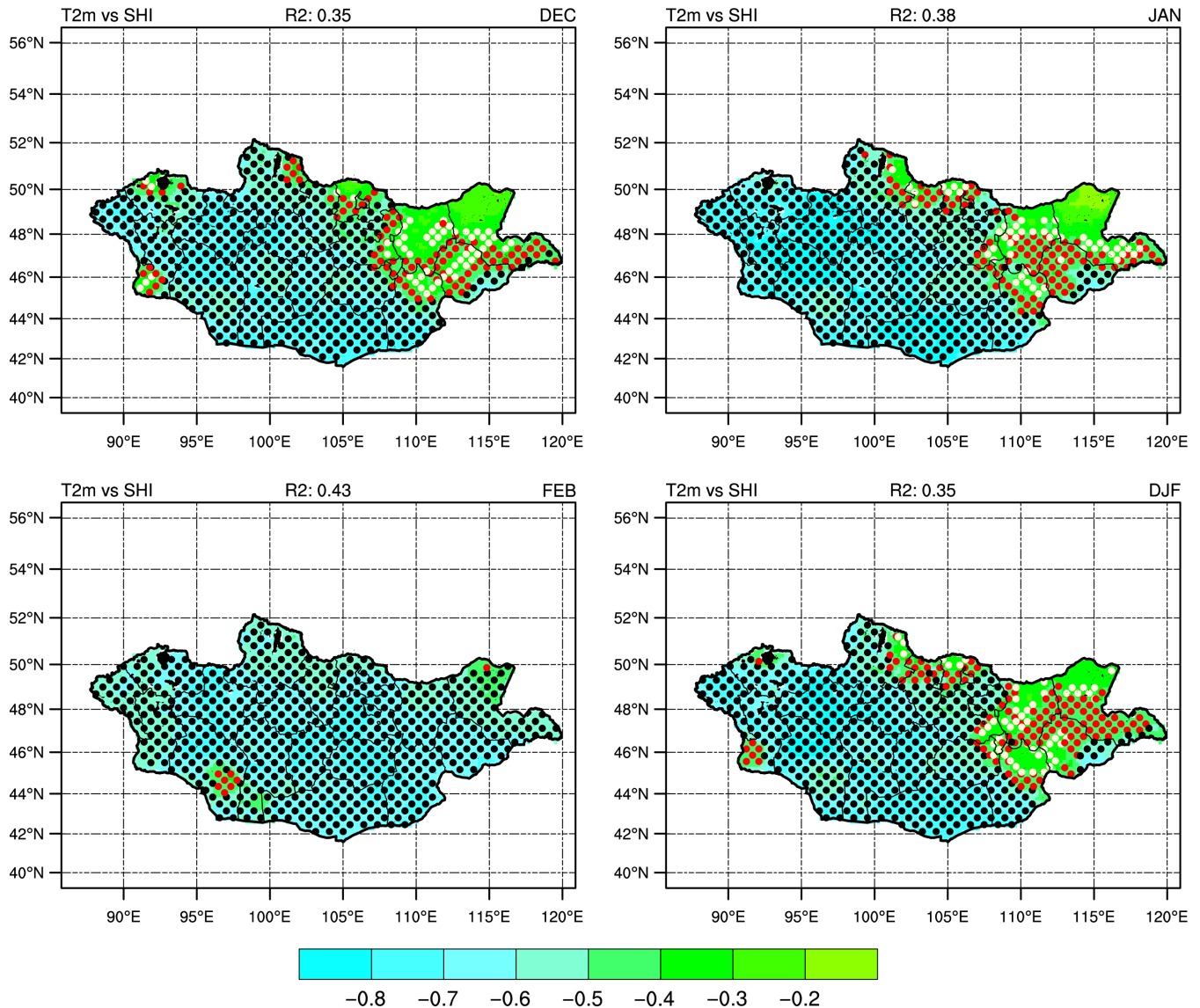


**FIGURE 3** Regression coefficients of aT2m ( $20 \times 20$  km grid) on the  $SHI_{obs}$ . Stippling with colours indicates statistical significances at 90% (white), 95% (red) and 99% (black) levels. R2 means the area-averaged coefficient of determinant [Colour figure can be viewed at [wileyonlinelibrary.com](http://wileyonlinelibrary.com)]

covered with ice during ASO. Considering both the correlations coefficients and ice coverages, we defined two ASO indices, the Barents–Kara Sea index (BKI) and the East Siberian Sea index (ESI), as SST and SIE anomalies averaged over the areas *A* and *P*, respectively, in order to analyse the relationship between the two ASO indices and the seasonal mean DJF  $TI_{obs}$  and  $SHI_{obs}$  series, and further to make use of the relationship in the prediction of T2m in Mongolia. These indices are independent of each other according to an independency test (i.e., the correlation coefficient between them is less than  $-0.04$ , which is statistically insignificant).

Thus, the contributions of impacts from these two ASO SST and SIE anomalies, BKI and ESI, on the anomalies of DJF temperature in Mongolia and the SH can be effectively combined by using MLR. Details of the MLR analysis of TI and SHI on the BKI and ESI, referred to as  $TI_{MLR}$  and  $SHI_{MLR}$ , respectively, are shown in Table 1. Both  $TI_{obs}$  and  $SHI_{obs}$  are significantly ( $p < .05$ ) related to both of the ASO

northern Kara Sea SST and Chukchi Sea SIE anomalies.  $TI_{MLR}$  and  $SHI_{MLR}$  are supported by the MLR results with the significance of the variances associated with the linear model against variances of residuals exceeding 99%, as shown by analysis of variance (ANOVA; Table 2). The determinant coefficients shown in Table 2 indicate that 66 and 44% of the total variance for  $TI_{obs}$  and  $SHI_{obs}$ , respectively, can be explained by the MLR model. This MLR analysis is performed on the dependent variables and the results suggest that the ASO BKI and ESI can be used as additional predictors together with CGCM prediction for the subsequent wintertime temperature anomalies in Mongolia.

#### 4 | METHODS

ANN, a nonlinear statistical technique (Benestad, 2001; Goyal *et al.*, 2012) applied for converting large-scale

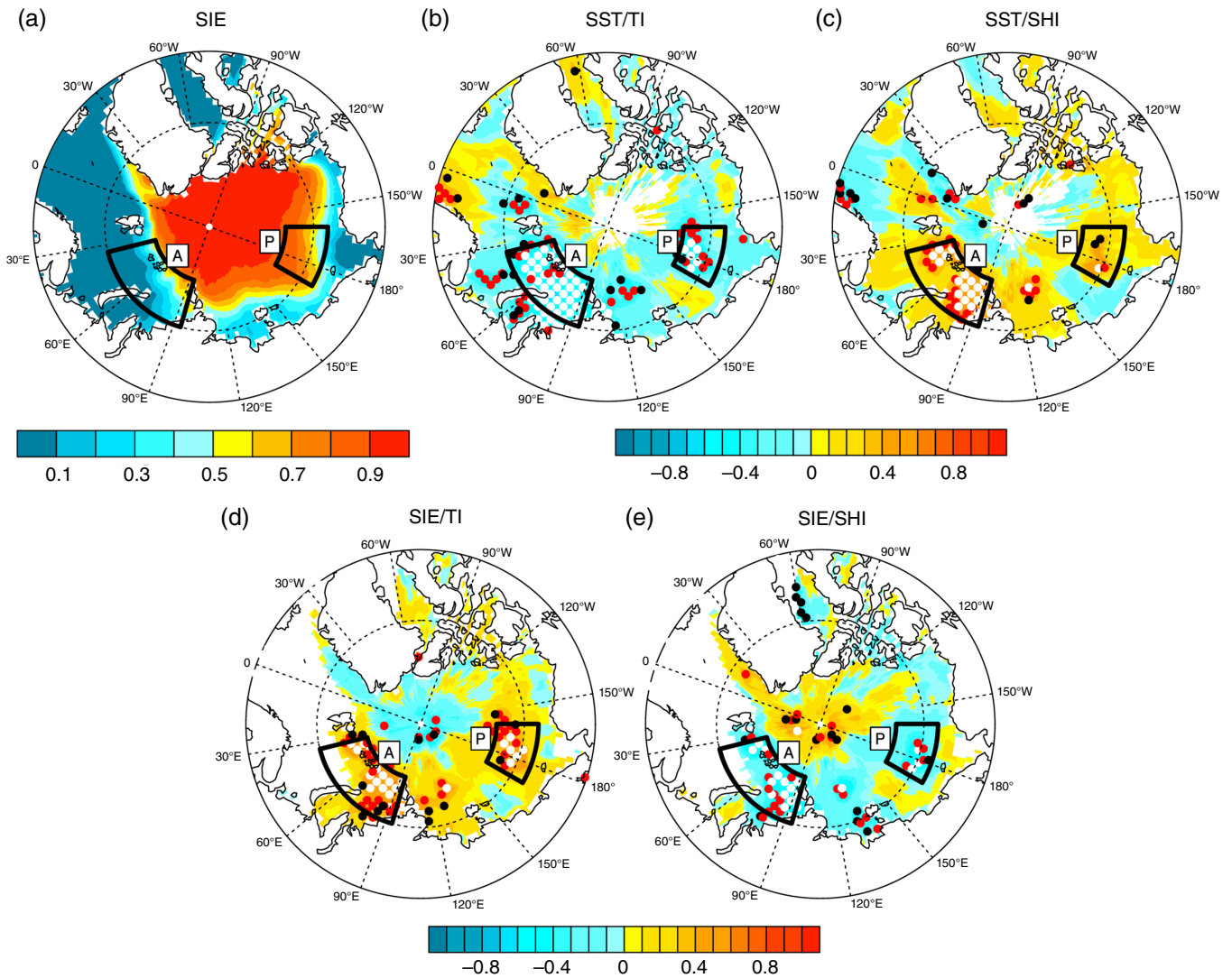


**FIGURE 4** Climatological SIE in the boreal early autumn (ASO) (a) and correlation coefficients between observed ASO SST and DJF  $TI_{obs}$  (b), and  $SHI_{obs}$  (c), and the correlation coefficients between observed ASO SIE and DJF  $TI_{obs}$  (d), and  $SHI_{obs}$  (e) during the period 1981–2014. Stippling with colours indicates statistically significant levels at 90% (black), 95% (red) and 99% (white) [Colour figure can be viewed at [wileyonlinelibrary.com](http://wileyonlinelibrary.com)]

**TABLE 1** MLR coefficients and their statistical characteristics for TI and SHI in DJF based on SST and SIE indices. BKI and ESI are SST and SIE anomalies averaged over the rectangular areas A ( $75^{\circ}$ – $82^{\circ}$ N and  $34^{\circ}$ – $94^{\circ}$ E) and P ( $73^{\circ}$ – $79^{\circ}$ N and  $170^{\circ}$ E– $160^{\circ}$ W), respectively

Model	$TI_{obs}$				$SHI_{obs}$			
	Coef.	SE	t	Sig.	Coef.	SE	t	Sig.
BKI	-0.75	0.12	-6.39	$3.5 \times 10^{-7}$	0.61	0.15	4.02	$3.3 \times 10^{-4}$
ESI	0.69	0.16	4.26	$1.7 \times 10^{-4}$	-0.58	0.21	-2.78	$8.8 \times 10^{-3}$

**TABLE 2** ANOVA for TI and SHI based on MLR against SST and SIE indices. Res, df and  $F$  stand for residual between observation and simulation, degree of freedom and  $F$  value for the model, respectively

Model	$TI_{MLR}$					$SHI_{MLR}$				
	Sum of squares	df	Mean square	$F$	Sig.	Sum of squares	df	Mean square	$F$	Sig.
Regrssion	23.6	2	11.8	30.6	$4.5 \times 10^{-8}$	15.8	2	7.90	12.43	$1.1 \times 10^{-4}$
Residual	11.9	31	0.38			19.8	31	0.64		
Total	35.5	33	1.1			35.7	33	1.1		
$R^2$	0.66					0.44				

variables into local-scale variables in some studies (e.g., Chadwick *et al.*, 2011), is also used in this study. Multilayer perceptron (Bishop, 1995), which is a supervised

learning method, is utilized for the statistical downscaling of the large-scale indices  $TI_{mdl}$ ,  $SHI_{mdl}$ ,  $TI_{MLR}$  and  $SHI_{MLR}$  to  $20 \times 20$  km horizontal resolution T2m. This is one of the

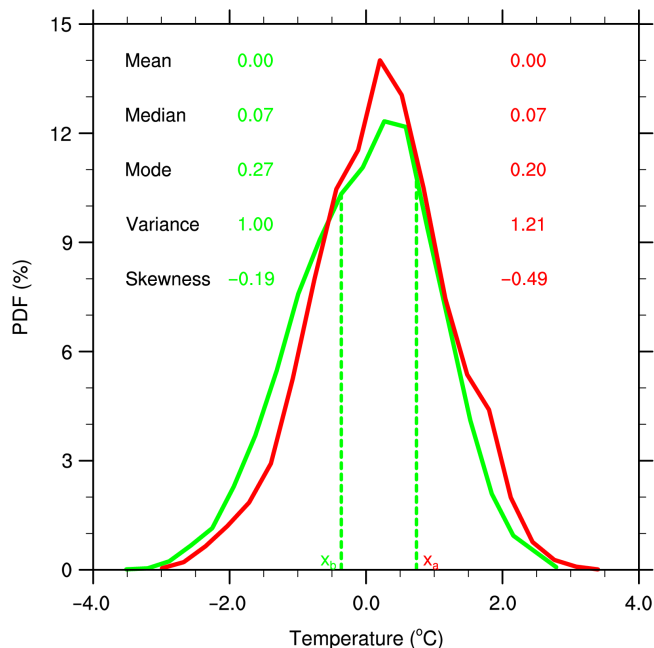


**FIGURE 5** PDFs of the observed (green) and predicted (red) aT2m during winter months over Mongolia. The  $X_a$  and  $X_b$  are plus and minus half of one standard deviation of the observed T2m, respectively [Colour figure can be viewed at wileyonlinelibrary.com]

most popular methods and known as a flexible type of neural network (Ahmed *et al.*, 2015). The ANN consists of input, hidden and output layers and has an activation function translating the input signal to the output one. The function makes the network nonlinear by determining the different weights between layers. Among the several activity functions, a hyperbolic tangent is used in this study. This function is commonly used in many studies because of its flexibility and fast convergence speed (Bhadeshia, 1999).

The ANN is performed for aT2m of  $20 \times 20$  km horizontal resolution over Mongolia using  $TI_{mdl}$ ,  $SHI_{mdl}$ ,  $TI_{MLR}$  and  $SHI_{MLR}$  as the input layers with a leave-one-out cross-validation (Michaelsen, 1987).

Although the  $20 \times 20$  km aT2m is deterministically obtained with the leave-one-out cross-validation, a probabilistic forecast is also performed for regional winter temperature over Mongolia. Richardson (2006) and Alessandri *et al.* (2011) introduced the advantage of probabilistic prediction and insisted that the seasonal climate predictions need to be probabilistic for more detailed information to the end users. Moreover, probability distribution functions (PDFs) for observed and predicted aT2m exhibit a close resemblance with a normal distribution (Figure 5). This implies that the basic characteristics of the observation and prediction are similar to each other. Thus, the boundaries of the three equiprobable categories (below, near and above normal) are defined in terms of the terciles of the normal distribution (Kharin and Zwiers, 2003). Since PDFs for observed and predicted aT2m have a normal distribution, the cumulative normal distribution function is evaluated to convert the deterministic forecast to a probabilistic forecast. Hence, the probabilities of aT2m prediction depend on the output of the ANN and the stochastic noise between predicted T2m and observed T2m.

## 5 | VERIFICATION

### 5.1 | Hindcast of PNU CGCM

The PNU CGCM T2m and SLP climatologies closely resemble the observations (not shown). Monthly and seasonal ensemble mean time series of  $TI_{mdl}$  and  $SHI_{mdl}$  are

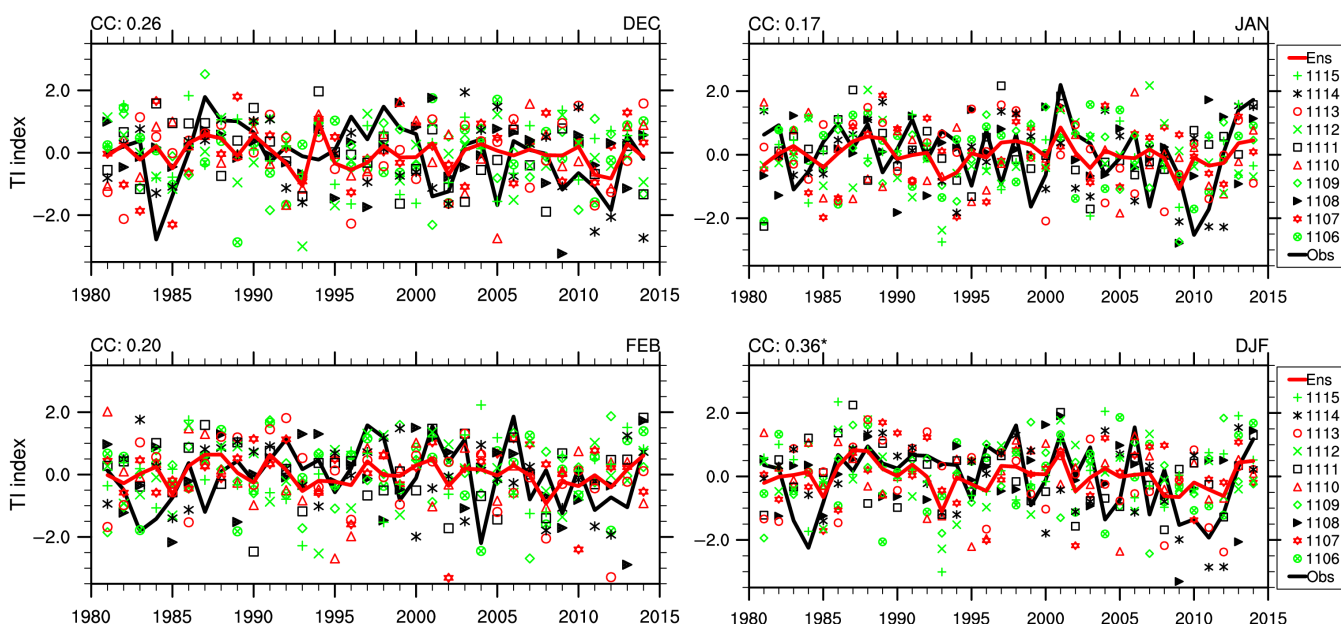


**FIGURE 6** Time series of observed and predicted TI derived from PNU CGCM with November initial condition. Solid black and red curves are observed and ensemble mean TI, respectively, and other colours with corresponding marks denote individual members. CC is correlation coefficient between observed and ensemble mean TI. The asterisk (\*) indicates statistical significance at 90% level [Colour figure can be viewed at wileyonlinelibrary.com]

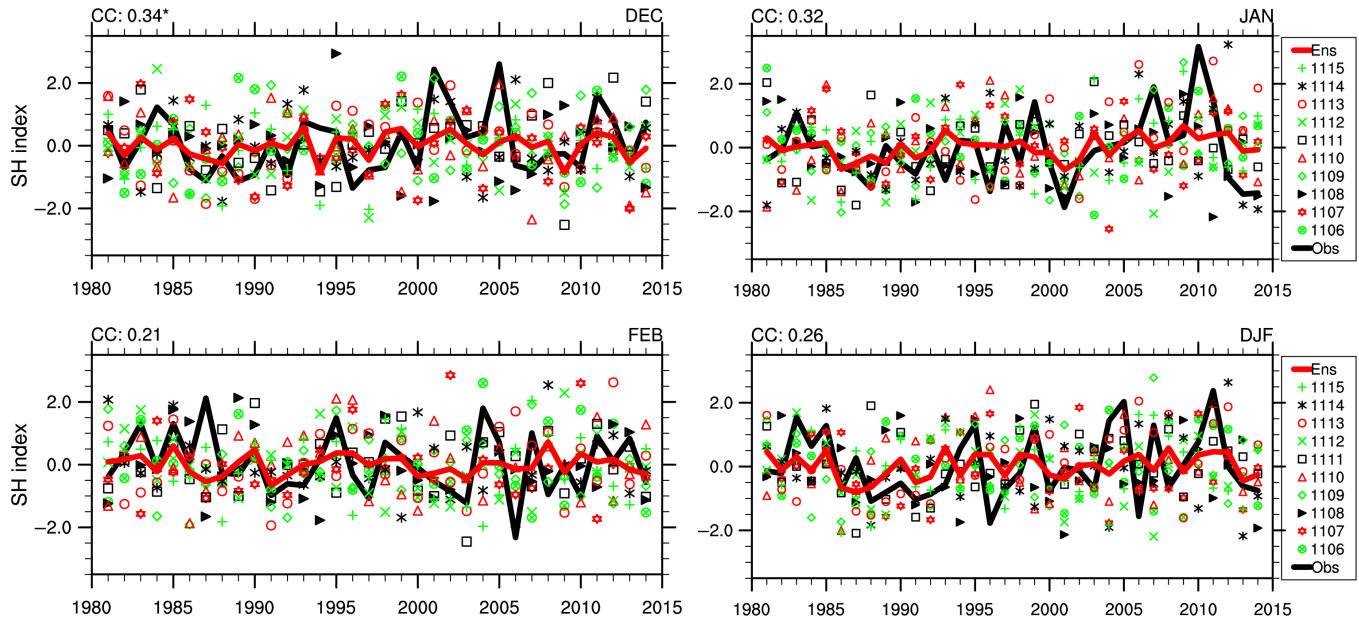


FIGURE 7 Same as Figure 6 but for SHI [Colour figure can be viewed at [wileyonlinelibrary.com](http://wileyonlinelibrary.com)]

correlated positively with the  $TI_{mdl}$  time series of  $TI_{obs}$  and  $SHI_{obs}$  (Figures 6 and 7), respectively. This implies that the model has some ability to predict large-scale indices such as  $TI_{mdl}$  and  $SHI_{mdl}$  with positive correlation within the range of 0.17–0.36. The correlation coefficients of each index decrease with increasing lead time, in general. Although all the coefficients between observation and hindcast of monthly and seasonal means of each index remain positive, only the correlation coefficients of seasonal mean DJF  $TI$  and DEC  $SHI$  exceed the 90% confidence level.

Even though the range of the correlation coefficients is similar to most of the state-of-the-art models and the multi-model ensemble predictions for the central Asia region (Min *et al.*, 2014; Kim *et al.*, 2016), this result indicates that the skill of seasonal predictions over the region is less reliable and not enough to meet the demand of the people and decision-makers of the region. Therefore, the aforementioned statistical approach using the ANN is necessary for better and horizontally finer prediction over the Mongolia region.

## 5.2 | ANN prediction

### 5.2.1 | $TI_{ANN}$ and $SHI_{ANN}$ predictions

The leave-one-out cross-validation is applied to the verification of all predictions, considering relatively short sample period of this study (1981–2015), that is described below. The large-scale indices  $TI_{ANN}$  and  $SHI_{ANN}$  and the  $20 \times 20$ -km-resolution T2m are predicted by means of the ANN with  $TI_{mdl}$  and  $SHI_{mdl}$ , and  $TI_{MLR}$  and  $SHI_{MLR}$  are incorporated as input layers. Anomaly correlation coefficients (ACC; WMO, 2002) between  $TI_{obs}$  ( $SHI_{obs}$ ) and outputs from  $TI_{mdl}$  ( $SHI_{mdl}$ ),  $TI_{MLR}$  ( $SHI_{MLR}$ ) and  $TI_{ANN}$  ( $SHI_{ANN}$ ) are listed in Table 3. The temporal correlation coefficients between the  $TI_{obs}$  ( $SHI_{obs}$ ) series and the estimated series are the highest when the ANN is used for most months and DJF

except  $TI_{ANN}$  in January and  $SHI_{ANN}$  in February and DJF. However, the ACC based on ANN in all months and DJF are statistically significant ( $p < .1$ ). The mean square skill scores (MSSS; WMO, 2002) for both large-scale indices are also presented in Table 3, which indicates that  $TI_{ANN}$  and  $SHI_{ANN}$  outperform the other seasonal predictions except  $TI_{ANN}$  in January and  $SHI_{ANN}$  in February and DJF.

### 5.2.2 | Predictions of the $20 \times 20$ -km-resolution T2m anomalies

Verification of the predictions of T2m anomalies at each  $20 \times 20$  km grid-point over Mongolia is performed in cross-

TABLE 3 ACC and MSSS between observed and predicted large-scale indices. Symbols \*, \*\* and \*\*\* indicate statistical significance at 90, 95 and 99% confidence levels, respectively

Index	Month	$TI_{mdl}/SHI_{mdl}$	$TI_{MLR}/SHI_{MLR}$	$TI_{ANN}/SHI_{ANN}$
<i>ACC</i>				
$TI_{obs}$	DEC	0.25	0.41**	0.45**
	JAN	0.17	0.41**	0.40**
	FEB	0.19	0.53***	0.54***
	DJF	0.36**	0.75***	0.76***
$SHI_{obs}$	DEC	0.30*	0.32*	0.35**
	JAN	0.33*	0.34**	0.34**
	FEB	0.20	0.42**	0.33*
	DJF	0.26	0.62***	0.60***
<i>MSSS</i>				
$TI_{obs}$	DEC	0.04	0.16	0.21
	JAN	−0.01	0.16	0.15
	FEB	−0.00	0.29	0.30
	DJF	0.12	0.59	0.61
$SHI_{obs}$	DEC	0.09	0.08	0.11
	JAN	0.12	0.13	0.11
	FEB	0.03	0.11	0.06
	DJF	0.06	0.31	0.33

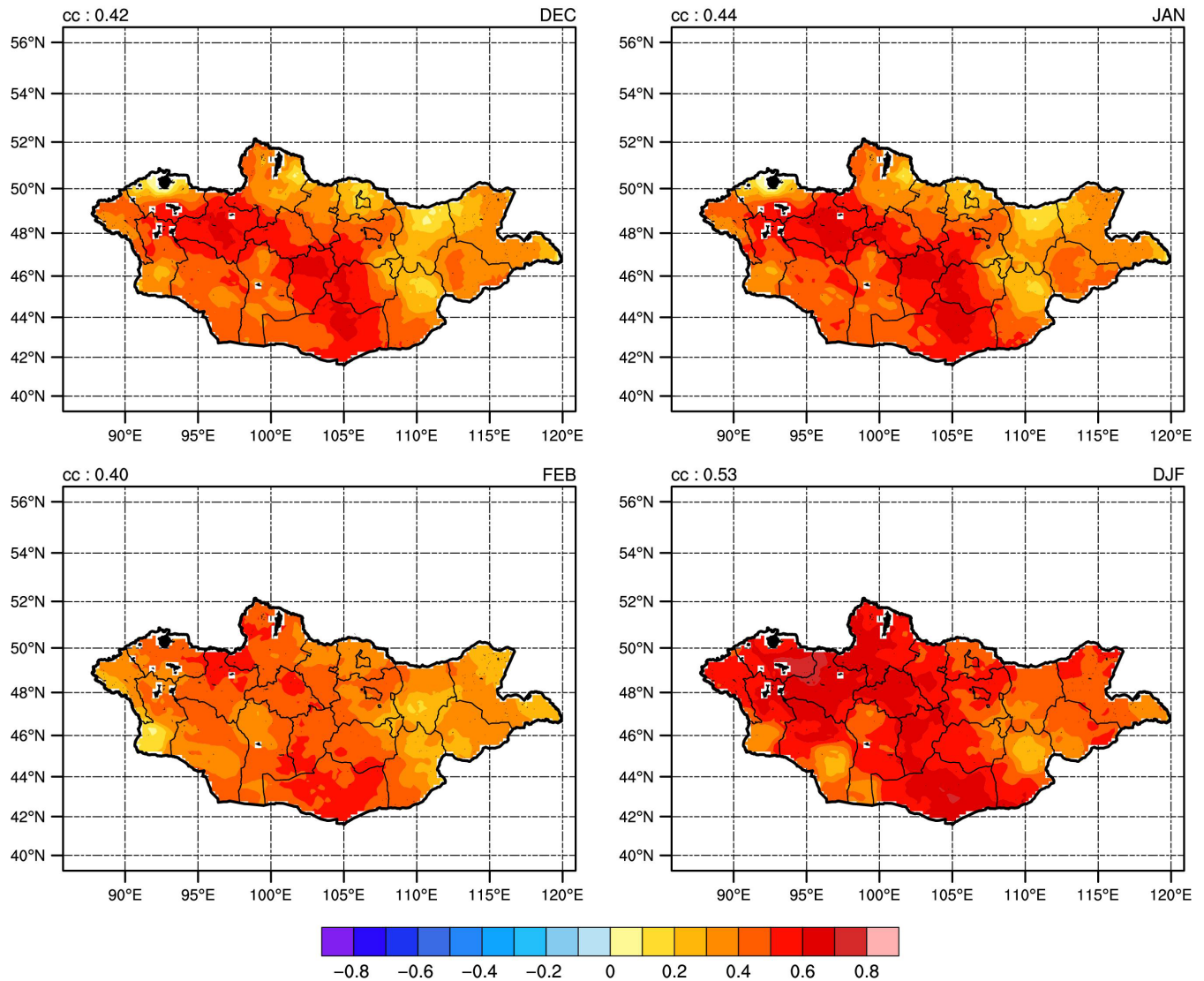


**FIGURE 8** ACC between observed and predicted  $20 \times 20$  km aT2m by ANN. CC stands for the area-averaged correlation coefficients [Colour figure can be viewed at [wileyonlinelibrary.com](http://wileyonlinelibrary.com)]

validation mode. The four predictors,  $TI_{mdl}$ ,  $SHI_{mdl}$ ,  $TI_{MLR}$  and  $SHI_{MLR}$ , predicted by the dynamical and statistical models are placed at the input layers of the ANN. The results are interpreted in both deterministic and probabilistic forms. For the latter, the predicted  $20 \times 20$  km T2m values are converted to tercile probabilities. For verification assessments we use ACC for deterministic forecasts and ranked probability skill score (RPSS) for probabilistic forecasts (Wilks, 1995).

The ACC between observed and predicted aT2m is shown in Figure 8. The correlations are all positive throughout the domain. However, the coefficients are relatively low over the southeastern Mongolia throughout the whole months and DJF and over the northeastern border of the country in December and January. The deterministic forecast of T2m demonstrates the high skill over most of Mongolia when ANN is used. For RPSS, a value of +1 indicates a perfect forecast, while a negative value means that the prediction skill is worse than the climatological forecast. In

Figure 9, although RPSS is generally better than the climatological forecast, negative RPSS values do exist in some regions of the domain. The ACC is higher in most of west and south Mongolia, whereas RPSS is higher in central and east Mongolia, especially in January and February, because the variation of T2m is relatively larger than that in eastern Mongolia. The ACC shows linear relationships between forecast and observations, while RPSS represents nonlinear relationships and skill with respect to the climatological forecast. Therefore, there is no close qualitative coincidence between Figures 8 and 9.

## 6 | SUMMARY AND CONCLUSION

In this study, the hindcast data of PNU CGCM, a participant model of the APCC multi-model ensemble climate prediction system, and ASO SST and SIE in the northern Kara Sea and Chukchi Sea, respectively, are used for

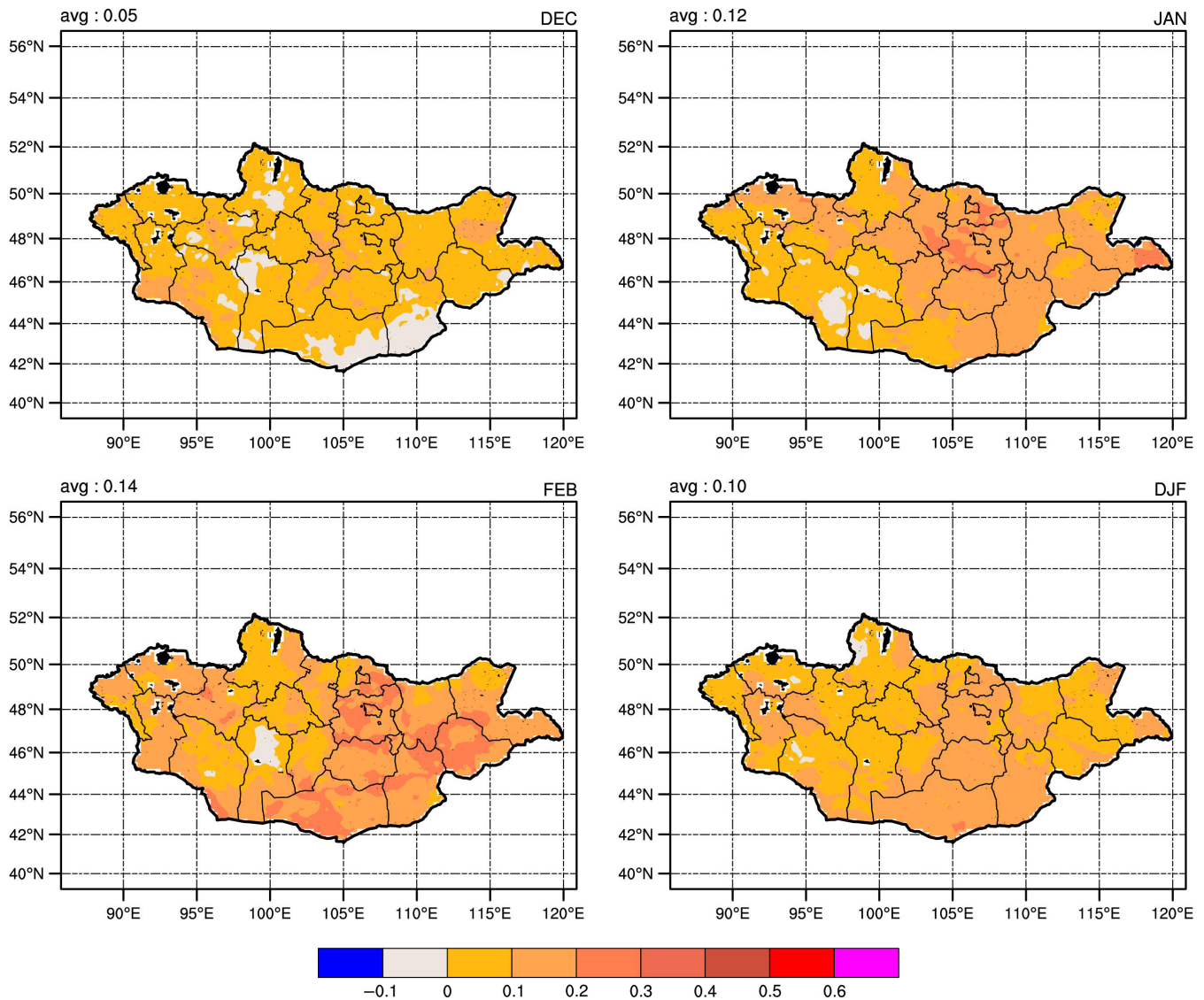


FIGURE 9 RPSS of the aT2m predictions. The avg stands for area-averaged RPSS [Colour figure can be viewed at [wileyonlinelibrary.com](http://wileyonlinelibrary.com)]

predicting  $20 \times 20$ -km-resolution aT2m over Mongolia for boreal winter. For this purpose, four area-averaged large-scale climate indices,  $TI_{mdl}$ ,  $SHI_{mdl}$ ,  $TI_{MLR}$  and  $SHI_{MLR}$ , are calculated using the CGCM and statistical method. The  $20 \times 20$ -km-resolution aT2m over Mongolia is predicted in terms of the large-scale indices under the assumption that the spatial distribution of T2m over Mongolia is directly influenced by the large-scale climate variability, although it is highly complicated by the complex geography.

The dynamical integration is performed using PNU CGCM for 0.5–2.5-month lead hindcasts for boreal winter with 10 ensemble members, based on a time-lagged method, from November of every year during the period 1981–2014. From the outputs of PNU CGCM,  $TI_{mdl}$  and  $SHI_{mdl}$  are acquired as the large-scale climate indices. Although the relationships between the hindcasted ( $TI_{mdl}$  and  $SHI_{mdl}$ ) and observed ( $TI_{obs}$  and  $SHI_{obs}$ ) indices during each month of winter and each season are consistent, the correlation does

not indicate that the dynamic prediction is capable of being used for operational seasonal forecast. In fact, even most of the state-of-the-art models and the multi-model ensemble prediction systems have relatively poor predictability in high-latitude landlocked regions such as the Eurasian continent (Min *et al.*, 2014; Kim *et al.*, 2016), compared to ocean areas. Thus, applying the result that both winter  $TI_{obs}$  and  $SHI_{obs}$  are significantly linearly related with ASO SST and SIE in the northern Kara Sea and Chukchi Sea, respectively, which are areas adjacent to the sea ice margin, MLR is performed for  $TI_{MLR}$  and  $SHI_{MLR}$  for each month and season using BKI and ESI indices. BKI and ESI are independent of each other and lead the targeted months for prediction by 2–6 months.

Then, the ANN method is applied to these four large-scale indices for the prediction and the statistical downscaling to  $20 \times 20$ -km-resolution aT2m over Mongolia. The ANN is performed with leave-one-out cross-validation for aT2m by putting the four large-scale indices,  $TI_{mdl}$ ,  $SHI_{mdl}$ ,

$TI_{MLR}$  and  $SHI_{MLR}$ , into the input layers. In setting up the ANN, monthly mean  $20 \times 20$ -km-resolution aT2m produced by Gerelchuluun and Ahn (2014) is utilized as observations.

The deterministic and probabilistic forecasts of aT2m over Mongolia are also evaluated. The probabilistic forecast is made from the deterministic form using the cumulative distribution function because the PDFs of the observed and predicted aT2m have similar normal distributions. The ACC and RPSS are also evaluated to validate the predictability of the deterministic and probabilistic forecasts, respectively. The results of both the deterministic prediction and the probabilistic prediction of T2m demonstrate that the method used in this study is sufficiently skilful for predicting the boreal winter temperature of  $20 \times 20$ -km-resolution over Mongolia. Our results show that the predictabilities of monthly and seasonal  $20 \times 20$ -km-resolution aT2m over Mongolia in winter are improved by applying the ANN method to  $TI_{mdl}$ ,  $SHI_{mdl}$ ,  $TI_{MLR}$  and  $SHI_{MLR}$ , compared to the case when only dynamic prediction is performed. Furthermore, according to the ACC and MSSS analyses, both  $TI_{ANN}$  and  $SHI_{ANN}$  also generally outperform the other predictions, such as  $TI_{mdl}$ ,  $SHI_{mdl}$ ,  $TI_{MLR}$  and  $SHI_{MLR}$ .

Because the ANN is a nonlinear statistical method, it is difficult to distinguish between the contribution of the CGCM result ( $TI_{mdl}$ ,  $SHI_{mdl}$ ) and the contribution of the observed SST and SIE ( $TI_{MLR}$ ,  $SHI_{MLR}$ ) to  $TI_{ANN}$ . However, given the relationship between the Mongolian winter climate and the CGCM prediction (Table 3), we can infer that  $TI_{ANN}$  must be more influenced by  $TI_{MLR}$  and  $SHI_{MLR}$ , although  $TI_{mdl}$  and  $SHI_{mdl}$  still exert a reasonable contribution.

## ACKNOWLEDGEMENTS

This work was carried out with the support of “Cooperative Research Program for Agriculture Science & Technology Development (Project No. PJ01229302),” Rural Development Administration and the Korea Meteorological Administration, Research and Development Program under Grant No. KMI2018-01213, Republic of Korea.

## ORCID

Gerelchuluun Bayasgalan  <http://orcid.org/0000-0002-2868-3056>

Joong-Bae Ahn  <http://orcid.org/0000-0001-6958-2801>

## REFERENCES

- Ahmed, K., Shahid, S., Haroon, S.B. and Xiao-Jun, W. (2015) Multilayer perceptron neural network for downscaling rainfall in arid region: a case study of Baluchistan, Pakistan. *Journal of Earth System Science*, 124(6), 1325–1341.
- Ahn, J.B. and Kim, H.J. (2014) Improvement of 1-month lead predictability of the wintertime AO using realistically varying solar constant for a CGCM. *Meteorological Applications*, 21, 415–418.
- Ahn, J.B. and Lee, J. (2016) A new multimodel ensemble method using nonlinear genetic algorithm: an application to boreal winter surface air temperature and precipitation prediction. *Journal of Geophysical Research: Atmospheres*, 121, 9263–9277. <https://doi.org/10.1002/2016JD025151>.
- Ahn, J.B., Lee, J. and Im, E.S. (2012) The reproducibility of surface air temperature over South Korea using dynamical downscaling and statistical correction. *Journal of the Meteorological Society of Japan*, 90(4), 493–507.
- Alessandri, A., Borrelli, A., Navarra, A., Arribas, A., Déqué, M.M., Rogel, P. and Weisheimer, A. (2011) Evaluation of probabilistic quality and value of the ENSEMBELS multimodel seasonal forecasts: comparison with DEMETER. *Monthly Weather Review*, 139, 581–607. <https://doi.org/10.1175/2010MWR3417.1>.
- Anderson, D.L.T., Stockdale, T., Balmaseda, M., Ferranti, L., Vitart, F., Molteni, F., Doblas-Reyes, F., Mogenson, K. and Vidard, A. (2007) Development of the ECMWF seasonal forecast system. *ECMWF Technical Memorandum*, 3, 503.
- Batbold, A., Sato, T., Ishikawa, M. and Jamba, T. (2011) Performance of dynamical downscaling for extreme weather event in eastern Mongolia: case study of severe windstorm on 26 May 2008. *Sola*, 7, 117–120.
- Benestad, R.E. (2001) A comparison between two empirical downscaling strategies. *International Journal of Climatology*, 21, 1645–1668.
- Bhadeshia, H.K.D.H. (1999) Neural networks in materials science. *ISIJ International*, 39, 966–979.
- Bishop, C.M. (1995) *Neural Networks for Pattern Recognition*. Oxford University Press: New York, 482 pp.
- Brankovic, C., Palmer, T.N., Molteni, F., Tibaldi, S. and Cubasch, U. (1990) Extended-range predictions with ECMWF models: time lagged ensemble forecasting. *Quarterly Journal of the Royal Meteorological Society*, 116, 867–912.
- Chadwick, R., Coppola, E. and Giorgi, F. (2011) An artificial neural network technique for downscaling GCM outputs to RCM special scale. *Nonlinear Processes in Geophysics*, 18, 1010–1028. <https://doi.org/10.5194/npg-18-1013-2011>.
- Chang, C.P., Liu, C.H. and Kuo, H.C. (2003) Typhoon Vamei: an equatorial tropical cyclone formation. *Geophysical Research Letters*, 30(3), 1150. <https://doi.org/10.1029/2002GL016365>.
- Chang, C.P., Harr, P.A. and Chen, H.J. (2005) Synoptic disturbances over the equatorial South China Sea and western maritime continent during boreal winter. *Monthly Weather Review*, 133, 489–503.
- Chogsom, D. (1964) *Some aspects of Dzud studies, geographical aspects in Mongolia*. Ulaanbaatar: Department of Hydrology and Meteorology Service of Mongolia.
- Coulibaly, P. and Dibike, Y.B. (2005) Downscaling precipitation and temperature with temporal neural networks. *Journal of Hydrology*, 6, 483–496.
- Derome, J., Lin, H. and Brunet, G. (2005) Seasonal forecasting with a simple general circulation model: predictive skill in the AO and PNA. *Journal of Climate*, 18, 597–609.
- Ding, Y. and Krishnamurti, T.N. (1987) Heat budget of the Siberian high and the winter monsoon. *Monthly Weather Review*, 115, 2428–2449.
- Gerelchuluun, B. and Ahn, J.B. (2014) Air temperature distribution over Mongolia using dynamical downscaling and statistical correction. *International Journal of Climatology*, 34, 2464–2476.
- Goyal, M.K., Ojha, C.S.P. and Donald, H.B. (2012) An evaluation of nonparametric statistical downscaling of temperature, precipitation and evaporation for semi-arid region in India. *ASCE-Journal of Hydrologic Engineering*, 17(5), 615–627. [https://doi.org/10.1061/\(ASCE\)HE.1943-5584.0000479](https://doi.org/10.1061/(ASCE)HE.1943-5584.0000479).
- Hall, R., Erdélyi, R., Hanna, E., Jones, J.M. and Scaife, A.A. (2015) Drivers of North Atlantic polar front jet stream variability. *International Journal of Climatology*, 35, 1697–1720.
- Henrik, F., Navarra, A. and Ward, M.N. (1999) Reduction of model systematic error by statistical correction for dynamical seasonal predictions. *Journal of Climate*, 12, 1974–1989.
- Honda, M., Inoue, J. and Yamane, S. (2009) Influence of low Arctic sea-ice minima on anomalously cold Eurasian winters. *Geophysical Research Letters*, 36, L08707. <https://doi.org/10.1029/2008GL037079>.
- Im, E.S., Ahn, J.B., Remedio, A.R. and Kwon, W.T. (2008) Sensitive of the regional climate of East/Southeast Asia to convective parameterizations in the RegCM3 modelling system. Part 1: focus on the Korean Peninsula. *International Journal of Climatology*, 28, 1861–1877.
- Kanamitsu, M., Ebisuzaki, W., Woollen, J., Yang, S., Hnilo, J.J., Fiorino, M. and Potter, G.L. (2002) NCEP–DOE AMIP-II reanalysis (R-2). *Bulletin of the*

- American Meteorological Society*, 83, 1631–1643. <https://doi.org/10.1175/BAMS-83-11-1631>.
- Kharin, V.V. and Zwiers, F.W. (2003) Improved seasonal probability forecast. *Journal of Climate*, 16, 1684–1701.
- Kim, H.J. and Ahn, J.B. (2015) Improvement in prediction of the Arctic Oscillation with a realistic ocean initial condition in a CGCM. *Journal of Climate*, 28, 8951–8967.
- Kim, G., Ahn, J.B., Kryjov, V.N., Sohn, S.J., Yun, W.T., Graham, R., Kolli, R. K., Kumar, A. and Ceron, J.J. (2016) Global and regional skill of the seasonal predictions by WMO Lead Center for Long-Range Forecast Multi-Model Ensemble. *International Journal of Climatology*, 36, 1657–1675.
- Kryjov, V.N. (2015) October circulation precursors of the wintertime Arctic Oscillation. *International Journal of Climatology*, 35, 161–171.
- Lee, D.Y., Ahn, J.B., Ashok, K. and Alessandri, A. (2013) Improvement of grand multi-model ensemble prediction skills for the coupled models of APCC/ENSEMBLES using a climate filter. *Atmospheric Science Letters*, 14, 139–145. <https://doi.org/10.1002/asl2.430>.
- Lee, D.Y., Ahn, J.B. and Yoo, J.H. (2014) Enhancement of seasonal prediction of East Asian summer rainfall related to western tropical Pacific convection. *Climate Dynamics*, 45, 1025–1042.
- Lin, H., Derome, J. and Brunet, G. (2005) Correction of atmospheric dynamical seasonal forecast using leading ocean-forced spatial pattern. *Geophysical Research Letters*, 32, L14804.
- MARCC. (2009) *Mongolia: assessment report on climate change*. Ulaanbaatar: MARCC.
- Meehl, G.A. (1995) Global coupled general circulation models. *Bulletin of the American Meteorological Society*, 76, 951–957.
- Michaelsen, J. (1987) Cross-validation in statistical climate forecast models. *Journal of Applied Meteorology*, 26, 1589–1600.
- Mijiddorj, R. (1999) *Atmospheric general circulation*. Ulaanbaatar: Photoffset, 138 pp.
- Min, Y.M., Kryjov, V.N. and Oh, S.M. (2014) Assessment of APCC multi-model ensemble prediction in seasonal climate forecasting: retrospective (1983–2003) and real-time forecasts (2008–2013). *Journal of Geophysical Research: Atmospheres*, 119(12), 12132–12150.
- Namkhai, A. and Mijiddorj, R. (1986) Drought frequency and unfavorable winter weather condition in Mongolia. *Proceedings of the IMH*, 11, 118–131.
- Natsagdorj, L. (2000) *Pastoral husbandry and Dzud, "Lessons from Dzud in 1999–2000"*. Ulaanbaatar: JEMR, pp. 48–82.
- Natsagdorj, L. and Dulamsuren, J. (2001) Some aspects of assessment of the Dzud phenomena. *Papers in Meteorology and Hydrology*, 23(3), 3–18.
- NCL. (2016) *The NCAR command language (version 6.3.0)*. Boulder, CO: UCAR/NCAR/CISL/TDD. <https://doi.org/10.5065/D6WD3XH5>.
- Orlanski, I. (1975) A rational subdivision of scales for atmospheric process. *Bulletin of the American Meteorological Society*, 56(5), 527–530.
- Panagiotopoulos, F., Shagedanova, M., Hannachi, A. and Stephenson, D. (2005) Observed trends and teleconnections of the Siberian high: a recently declining center of action. *Journal of Climate*, 18(9), 1411–1422.
- Park, T.W., Ho, C.H. and Deng, Y. (2014) A synoptic and dynamical characterization of wave-train and blocking cold surge over East Asia. *Climate Dynamics*, 43, 753–770. <https://doi.org/10.1007/s00382-013-1817-6>.
- Rayner, N.A., Brohan, P., Parker, D.E., Folland, C.K., Kennedy, J.J., Vanicek, M., Ansell, T. and Tett, S.F.B. (2006) Improved analyses of changes and uncertainties in sea surface temperature measured in situ since the mid-nineteenth century: the HadSST2 data set. *Journal of Climate*, 19(3), 446–469.
- Richardson, D.S. (2006) Predictability and economic value. In: Palmer, T. and Hagedorn, R. (Eds.) *Predictability of Weather and Climate*. Cambridge: Cambridge University Press, pp. 628–644. <https://doi.org/10.1017/CBO9780511617652.026>.
- Scaife, A.A., Arribas, A., Blockley, E., Brookshaw, A., Clark, R.T., Dunstone, N., Eade, R., Fereday, D., Folland, C.K., Gordon, M., Hermanson, L., Knight, J.R., Lea, D.J., MacLachlan, C., Maidens, A., Martin, M., Peterson, A.K., Smith, D., Vellinga, M., Wallace, E., Waters, J. and Williams, A. (2014) Skillful long-range prediction of European and North American winters. *Geophysical Research Letters*, 41, 2514–2519. <https://doi.org/10.1002/2014GL059637>.
- Schoof, J.T. and Pryor, S.C. (2001) Downscaling temperature and precipitation: a comparison of regression-based methods and artificial neural networks. *International Journal of Climatology*, 21, 773–790.
- Sun, J. and Ahn, J.B. (2014) Dynamical seasonal predictability of the Arctic Oscillation using a CGCM. *International Journal of Climatology*, 35, 1342–1353.
- Sun, J. and Chen, H. (2012) A statistical downscaling scheme to improve global precipitation forecasting. *Meteorology and Atmospheric Physics*, 117, 87–102. <https://doi.org/10.1007/s00703-012-0195-7>.
- Toth, Z., Zhu, Y. and Marchok, T. (2001) The use of ensembles to identify forecasts with small and large uncertainty. *Bulletin of the American Meteorological Society*, 16, 463–477.
- Wigley, T.M.L., Jones, P.D., Briffa, K.R. and Smith, G. (1990) Obtaining sub-grid-scale information from coarse-resolution general circulation model output. *Journal of Geophysical Research*, 95(D2), 1943–1953. <https://doi.org/10.1029/JD095iD02p01943>.
- Wilks, D.S. (1995) *Statistical Methods in the Atmospheric Sciences*. Academic Press: New York, p. 467.
- WMO. (2002) Standardized verification system for long-range forecast. In: *Manual on the GDPS*, Vol. 1. Geneva: WMO, WMO-No. 485.
- Wu, B., Zhang, R. and D'Arrigo, R. (2006) Distinct modes of the East Asian winter monsoon. *Monthly Weather Review*, 134(8), 2165–2179.
- Wu, B.Y., Su, J.Z. and Zhang, R.H. (2011) Effects of autumn–winter Arctic sea ice on winter Siberian high. *Chinese Science Bulletin*, 56, 3220–3228. <https://doi.org/10.1007/s11434-011-4696-4>.

**How to cite this article:** Bayasgalan G, Ahn J-B. Seasonal prediction of high-resolution temperature at 2-m height over Mongolia during boreal winter using both coupled general circulation model and artificial neural network. *Int J Climatol*. 2018;1–12. <https://doi.org/10.1002/joc.5848>